ELSEVIER

Journal of Computational and Applied Mathematics 50 (1994) 523–532

JOURNAL OF COMPUTATIONAL AND APPLIED MATHEMATICS

A nonlinear truck model and its treatment as a multibody system *

B. Simeon [a,*], F. Grupp [b], C. Führer [b], P. Rentrop [a]

[a] *Mathematisches Institut, Technische Universität München, D-80290 München, Germany*
[b] *Laboratory for Robotics and System Dynamics, German Aerospace Research Establishment, D-82230 Wessling, Germany*

Received 27 July 1992; revised 2 December 1992

Abstract

A planar vertical truck model with nonlinear suspension and its multibody system formulation are presented. The equations of motion of the model form a system of differential-algebraic equations (DAEs). All equations are given explicitly, including a complete set of parameter values, consistent initial values, and a sample road excitation. Thus the truck model allows various investigations of the specific DAE effects and represents a test problem for algorithms in control theory, mechanics of multibody systems, and numerical analysis. Several numerical tests show the properties of the model.

Key words: Truck model; Differential-algebraic equations; Multibody systems

1. Introduction

The simulation of mechanical systems is a field of current research in both applied mathematics and mechanical engineering. Particularly in robotics and vehicle dynamics, the multibody system approach provides an efficient tool for the design and analysis process. The mechanical system is represented as a system of rigid or elastic bodies and massless interconnections. Modern computer programs, socalled *multibody formalisms*, generate the equations of motion

$$\begin{aligned} \dot{p} &= v, \\ M(p,t)\dot{v} &= f(p,v,t) - G(p,t)^{\mathrm{T}}\lambda, \\ 0 &= g(p,t), \end{aligned} \tag{1}$$

* This work has been supported by the Stiftung Volkswagenwerk within the general program Fachübergreifende Gemeinschaftsprojekte in den Ingenieurwissenschaften.

* Corresponding author. e-mail: bernd.simeon@mathematik.tu-muenchen.de.

SSDI 0377-0427(93)E0148-F

for the unknown n_p position coordinates $p(t)$ and n_p velocity coordinates $v(t)$. $M(p, t) \in \mathbb{R}^{n_p, n_p}$ denotes the symmetric positive definite mass matrix, the vector $f(p, v, t) \in \mathbb{R}^{n_p}$ the applied forces, $g(p, t) \in \mathbb{R}^{n_\lambda}$, $n_\lambda < n_p$, the holonomic constraints, $\lambda(t) \in \mathbb{R}^{n_\lambda}$ the generalized constraint forces and $G(p, t) := (\partial/\partial p)g(p, t)$.

In mathematical terms, the Lagrange equations of the first kind (1) form a system of *differential-algebraic equations (DAEs) of index* 3. Formula (1) is redundant since it is not reduced to the *state space form* which is characterized by a minimum set of coordinates and a system of ordinary differential equations (ODEs). Unfortunately, this reduction is not always feasible, especially for systems with closed loops, and may require substantial analytical work. While there are efficient and reliable numerical methods for state space formulations, the development of the corresponding tools for the DAE formulation or *descriptor form* (1) is a focus of current research. The high index of (1) causes serious problems for the numerical integration [2,6,9]. The alternative differentiation of the constraint equations lowers the index and results in index-2 and index-1 systems. Especially for the latter system, a variety of numerical integration methods is available but the results obtained in this way show large deviations in the original position constraints — the *drift phenomenon*.

The planar truck model presented in this paper is used by engineers both for a ride quality investigation and a driving safety analysis by means of the variations of the contact forces between the tires and the road. It forms a multibody system with seven bodies, linear and nonlinear suspension elements, and a kinematic joint. The equations of motion are introduced in Section 2. They yield a system of 23 differential-algebraic equations including one holonomic constraint. A state space formulation follows immediately from the choice of the coordinate system. Thus all results of the DAE case can be related to the ODE case.

The truck model enables thorough investigations of the particular DAE effects. In Section 3, numerical experiments show both the failure of BDF methods when applied to the index-3 formulation and the drift in case of the index-1 formulation. Numerical stabilization techniques are discussed. The dimension and the bad scaling of the model, which is typical for problems in vehicle dynamics, require a careful treatment.

2. Equations of motion of the truck model

Fig. 1 shows the complete multibody system representation of the truck with coordinates, bodies and force elements. The model is planar and consists of

body 1: rear tire, body 2: front tire, body 3: truck chassis, body 4: engine,
body 5: driver cabin, body 6: driver seat, body 7: loading area and load.

The truck proceeds with constant speed v_0. External forces are the driveway excitation $u(t)$ acting on the tires and the gravitational force. The $n_p = 11$ coordinates describe the displacements and rotations of the system with respect to the static equilibrium position:

p_1: vertical motion of rear tire, p_2: vertical motion of front tire,
p_3: vertical motion of truck chassis, p_4: rotation about y-axis of truck chassis,
p_5: vertical motion of engine, p_6: rotation about y-axis of engine,

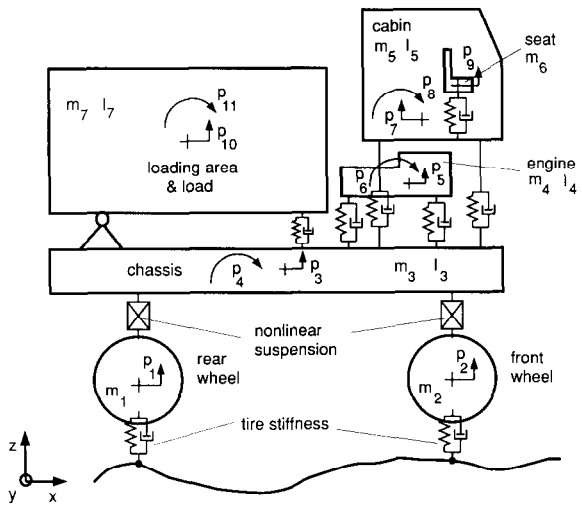

Fig. 1. Coordinates of the multibody system.

p_7: vertical motion of driver cabin, p_8: rotation about y-axis of driver cabin,

p_9: vertical motion of driver seat, p_{10}: vertical motion of loading area,

p_{11}: rotation about y-axis of loading area.

Using the Newton and Euler equations and the assumption that all forces act only in vertical direction, the equations of motion read

$$
\begin{aligned}
&m_1\ddot{p}_1 = -F_{10} + F_{13} - m_1 g_{\mathrm{erd}},\\
&m_2\ddot{p}_2 = -F_{20} + F_{23} - m_2 g_{\mathrm{erd}},\\
&m_3\ddot{p}_3 = -F_{13} - F_{23} + F_{35} + F_{34} + F_{43} + F_{53} + F_{37} - m_3 g_{\mathrm{erd}} + F_{z_3},\\
&l_3\ddot{p}_4 = (a_{23}F_{23} - a_{13}F_{13} - a_{37}F_{37} - a_{34}F_{34} - a_{35}F_{35} - a_{43}F_{43} - a_{53}F_{53})\cos\, p_4 + M_{z_4},\\
&m_4\ddot{p}_5 = -F_{43} - F_{34} - m_4 g_{\mathrm{erd}},\\
&l_4\ddot{p}_6 = (b_{43}F_{43} - b_{34}F_{34})\cos\, p_6,\\
&m_5\ddot{p}_7 = -F_{53} - F_{35} + F_{56} - m_5 g_{\mathrm{erd}},\\
&l_5\ddot{p}_8 = (c_{53}F_{53} - c_{35}F_{35} - c_{56}F_{56})\cos\, p_8,\\
&m_6\ddot{p}_9 = -F_{56} - m_6 g_{\mathrm{erd}},\\
&m_7\ddot{p}_{10} = -F_{37} - m_7 g_{\mathrm{erd}} + F_{z_{10}},\\
&l_7\ddot{p}_{11} = e_{37}\cos\, p_{11}F_{37} + M_{z_{11}},
\end{aligned}
\tag{2}
$$

where F_{ij} denotes the force acting between body i and body j and F_{z_3}, M_{z_4}, $F_{z_{10}}$, $M_{z_{11}}$ the constraint forces due to the joint between body 7 and body 3. This holonomic constraint is expressed by the algebraic equation

$$
0 = g(p) = -p_3 - a_{z_1}\sin\, p_4 - a_{z_2}\cos\, p_4 + p_{10} + e_{z_1}\sin\, p_{11} - e_{z_2}\cos\, p_{11} + h_{\mathrm{eq}}. \tag{3}
$$

h_{eq} denotes the distance between the center of the chassis and the center of the load in the static equilibrium position. Thus $n_\lambda = 1$, and the constraint matrix is given by $G = \mathrm{d}g(p)/\mathrm{d}p$.

The forces are defined by

$$
\begin{aligned}
&F_{10} = k_{10}x_{10}(t) + d_{10}\dot{x}_{10}(t) - F_{eq,10}, && F_{20} = k_{20}x_{20}(t) + d_{20}\dot{x}_{20}(t) - F_{eq,20},\\
&F_{13} = f_{13}(x_{13}(t)) + d_{13}\dot{x}_{13}(t), && F_{23} = f_{23}(x_{23}(t)) + d_{23}\dot{x}_{23}(t),\\
&F_{34} = k_{34}x_{34}(t) + d_{34}\dot{x}_{34}(t) - F_{eq,34}, && F_{43} = k_{43}x_{43}(t) + d_{43}\dot{x}_{43}(t) - F_{eq,43},\\
&F_{35} = k_{35}x_{35}(t) + d_{35}\dot{x}_{35}(t) - F_{eq,35}, && F_{53} = k_{53}x_{53}(t) + d_{53}\dot{x}_{53}(t) - F_{eq,53},\\
&F_{56} = k_{56}x_{56}(t) + d_{56}\dot{x}_{56}(t) - F_{eq,56}, && F_{37} = k_{37}x_{37}(t) + d_{37}\dot{x}_{37}(t) - F_{eq,37},
\end{aligned}
\tag{4}
$$

where f_{13} and f_{23} represent nonlinear spring laws (see the Appendix) and

$$
\begin{aligned}
x_{10} &= p_1 - u(t - t_1),\\
x_{20} &= p_2 - u(t - t_2),\\
x_{13} &= p_3 + a_{13}\sin p_4 - p_1,\\
x_{23} &= p_3 - a_{23}\sin p_4 - p_2,\\
x_{34} &= p_5 + b_{34}\sin p_6 - p_3 + a_{34}\sin p_4,\\
x_{43} &= p_5 - b_{43}\sin p_6 - p_3 + a_{43}\sin p_4,\\
x_{35} &= p_7 + c_{35}\sin p_8 - p_3 + a_{35}\sin p_4,\\
x_{53} &= p_7 - c_{53}\sin p_8 - p_3 + a_{53}\sin p_4,\\
x_{56} &= p_9 - p_7 + c_{56}\sin p_8,\\
x_{37} &= p_{10} - e_{37}\sin p_{11} - e_{z2}\cos p_{11} - p_3 + a_{37}\sin p_4,\\
\dot{x}_{10} &= \dot{p}_1 - \dot{u}(t - t_1),\\
\dot{x}_{20} &= \dot{p}_2 - \dot{u}(t - t_2),\\
\dot{x}_{13} &= \dot{p}_3 + a_{13}\dot{p}_4\cos p_4 - \dot{p}_1,\\
\dot{x}_{23} &= \dot{p}_3 - a_{23}\dot{p}_4\cos p_4 - \dot{p}_2,\\
\dot{x}_{34} &= \dot{p}_5 + b_{34}\dot{p}_6\cos p_6 - \dot{p}_3 + a_{34}\dot{p}_4\cos p_4,\\
\dot{x}_{43} &= \dot{p}_5 - b_{43}\dot{p}_6\cos p_6 - \dot{p}_3 + a_{43}\dot{p}_4\cos p_4,\\
\dot{x}_{35} &= \dot{p}_7 + c_{35}\dot{p}_8\cos p_8 - \dot{p}_3 + a_{35}\dot{p}_4\cos p_4,\\
\dot{x}_{53} &= \dot{p}_7 - c_{53}\dot{p}_8\cos p_8 - \dot{p}_3 + a_{53}\dot{p}_4\cos p_4,\\
\dot{x}_{56} &= \dot{p}_9 - \dot{p}_7 + c_{56}\dot{p}_8\cos p_8,\\
\dot{x}_{37} &= \dot{p}_{10} - e_{37}\dot{p}_{11}\cos p_{11} + e_{z2}\dot{p}_{11}\sin p_{11} - \dot{p}_3 + a_{37}\dot{p}_4\cos p_4.
\end{aligned}
\tag{5}
$$

$k_{10},\ldots,k_{56}$ $d_{10},\ldots,d_{56}$ denote stiffness and damping coefficients while a_*, b_*, c_*, e_* are geometry constants. $F_{eq,10},\ldots,F_{eq,56}$ represent the nominal forces which can be obtained from the static equilibrium position $p = \dot{p} = \ddot{p} = 0$. This leads to a system of linear equations in $F_{eq,10},\ldots,F_{eq,56}$ and λ. The values of these constant parameters are given in the Appendix.

A final transformation

$$\dot{p} = v$$

into a system of first order yields the standard form (1). In this descriptor representation, the equations of motion of the truck model form a differential-algebraic system of index 3.

In order to derive a state space formulation, the constraint equation (3) is solved for the coordinate p_{10}. The expressions p_{10}, $\dot{p}_{10}$, $\ddot{p}_{10}$ are then substituted into the equations of motion (2). Since

$$m_7 \ddot{p}_{10} = -F_{37} - m_7 g_{\text{erd}} - \lambda,$$

we can eliminate the Lagrange multiplier λ. Finally, the expression for λ is inserted in the dynamic equations for p_3, p_4, p_{11}, which results in the reduced equations of motion.

Remark. This straightforward choice of a set of minimum coordinates leads to a *mass matrix which depends on the coordinates and is nondiagonal, while the mass matrix of the descriptor form is constant and diagonal.* Thus both the choice of the coordinates and the formulation in descriptor or state space form strongly influence the computational complexity of the equations of motion. Obviously, any numerical algorithm which exploits the structure of the equations profits from a constant and diagonal mass matrix.

3. Numerical integration of the truck model

In a first attempt, the truck model was integrated by the DAE code DASSL [2], a multistep method based on the backward differentiation formulas (BDFs), in the semi-explicit index-3 formulation

$$\dot{p} = v, \tag{6a}$$

$$\dot{v} = w, \tag{6b}$$

$$0 = Mw - f(p, v, t) + G(p)^{\mathrm{T}}\lambda, \tag{6c}$$

$$0 = g(p), \tag{6d}$$

where the variables $w \in \mathbb{R}^{n_p}$ stand for the accelerations in the system. Fig. 2 shows what happened already after a few steps with prescribed tolerances RTOL $= 10^{-3}$, ATOL $= 10^{-4}$ for the variables p, v, w and RTOL $= 10^{-3}$, ATOL $= 1$ for λ. The step size h is reduced up to almost machine precision and finally the integration breaks down since the corrector iteration does not converge. The reason for this failure is the high index 3 of (6). DASSL was written for index-1 systems, in case of a higher index the approximation of some variables, here v, w, λ, suffers from an order reduction which causes the stepsize control to break down [2].

To lower the index to 1, the constraint (6d) is now differentiated twice, and DASSL is applied again. Fig. 3 illustrates the numerical problems if this formulation is employed for the integration. Obviously, the numerical solution only satisfies the twice differentiated constraint. Increasing with time t, it deviates considerably from the original position constraint (6d) — the so-called *drift off*. Depending on the problem and the integration interval, this instability may

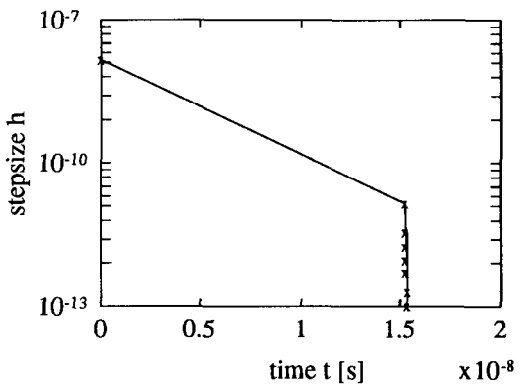

Fig. 2. Stepsize reduction of index-3 system.

completely falsify the numerical results [9]. For the truck model and the above integration interval, the drift shows the typical quadratic increase.

Several approaches have been introduced in order to stabilize the integration process, see [3] for a survey. Fig. 4 shows the result of an integration run by the code ODASSL [4], a modified version of DASSL. ODASSL uses the position constraint (6d) and, in addition, the once and twice differentiated constraints in order to stabilize the integration process. The resulting *overdetermined system* of equations is discretized with the BDFs. Now, the corrector step for the numerical solution is defined by an overdetermined nonlinear algebraic system. Its solution in a certain least-squares sense can be interpreted as a numerical projection onto the constraint manifold. For the same purpose, an analytical projection based on the underlying variational calculus is derived in [8]. Other special integration methods for higher-index DAEs and constrained mechanical systems are discussed in [1,6,7].

In Fig. 4, the tolerances were set to RTOL $= 10^{-4}$, ATOL $= 10^{-5}$ for the variables p, v, w and to RTOL $= 10^{-4}$, ATOL $= 10^{-1}$ for λ. For a realistic simulation run, a Fourier series approximation of driveway measurements with an additional exponential damping factor was used as excitation $u(t)$. The response of the driver seat can still be optimized by a tuning of the

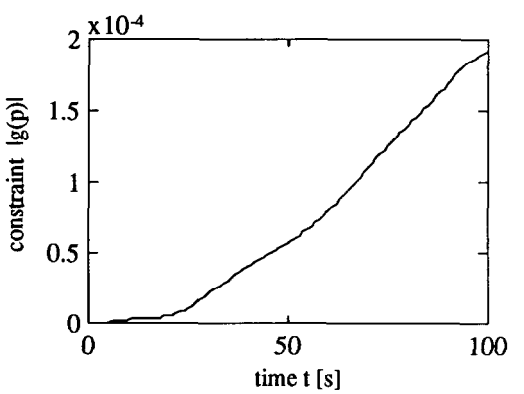

Fig. 3. Drift effect of index-1 system.

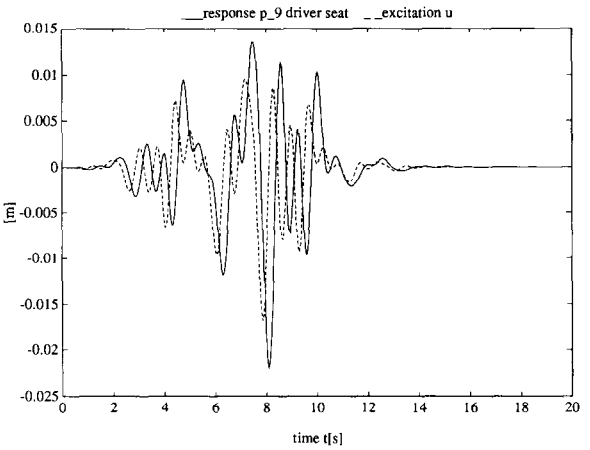

Fig. 4. Approximation of road excitation u, response of seat p_9 and integration statistics of ODASSL. (Number of steps = 1193; number of function evaluations = 2403; number of Jacobian evaluations = 14; number of error test failures = 4; CPU = 44.5 (workstation Apollo DN4500).)

suspension. Note that ODASSL keeps the drift well below a certain tolerance and returns a very accurate solution for all variables p, v, w, λ.

Finally, it should be stressed that the truck model is badly scaled since the constraint force λ is of magnitude 10^4 while the displacements are of magnitude 10^{-2}. This is typical for problems in vehicle system dynamics. The bad scaling leads to very large condition numbers of the iteration matrix inside DASSL and ODASSL (Table 1) — the integration breaks down for very stringent tolerances. In order to avoid this problem, the constraint force λ is scaled by a factor of 10^{-6}. All of the above experiments were performed with this scaling.

4. Conclusion

The truck example presented in this paper enables thorough investigations of the particular DAE effects in multibody system dynamics. Its dimension and its bad scaling require a careful treatment. Numerical integration methods as well as algorithms for the identification of system parameters and for a suspension optimization in terms of active controllers can be tested. The latter problems are investigated in [5].

All results obtained from the DAE formulation can be related to the results in the ODE case since the state space formulation is available. This is a clear advantage of the truck example.

Table 1
Condition numbers of the iteration matrix depending on the stepsize h; the index-1 system is written as $F(t, y, \dot{y}) = 0$, $y = [p, v, w, \lambda]$

$\mathrm{cond}(F_{\dot{y}}/h + F_y)$	$h = 10^{-1}$	$h = 10^{-3}$	$h = 10^{-5}$	$h = 10^{-7}$
Unscaled	$1.9 \cdot 10^{12}$	$7.5 \cdot 10^{10}$	$2.1 \cdot 10^{12}$	$2.2 \cdot 10^{14}$
Scaled	$5.4 \cdot 10^{7}$	$7.9 \cdot 10^{5}$	$2.0 \cdot 10^{7}$	$2.2 \cdot 10^{9}$

Moreover, a linearized version is derived easily. A MATLAB input file with the matrices of the linearized model as well as a FORTRAN77 subroutine for the evaluation of the nonlinear equations of motion can be obtained from the authors.

Appendix. Technical parameters

Truck parameters

The masses m_i and moments of inertia l_i are

body 1: rear tire: $m_1 = 1450$ kg,
body 2: front tire: $m_2 = 600$ kg,
body 3: chassis: $m_3 = 1980$ kg, $l_3 = 10\,367$ kgm^2,
body 4: engine: $m_4 = 1355$ kg, $l_4 = 432$ kgm^2,
body 5: cabin: $m_5 = 1000$ kg, $l_5 = 948$ kgm^2,
body 6: seat: $m_6 = 100$ kg,
body 7: load: $m_7 = 11\,515$ kg, $l_7 = 33\,000$ kgm^2.

The stiffness k_i and damping d_i coefficients are

$k_{10} = 4\,400\,000$ N/m, $d_{10} = 600$ Ns/m,
$k_{20} = 2\,200\,000$ N/m, $d_{20} = 300$ Ns/m,
$k_{34} = 2\,643\,833$ N/m, $d_{34} = 618$ Ns/m,
$k_{43} = 779\,735$ N/m, $d_{43} = 182$ Ns/m,
$k_{35} = 135\,707$ N/m, $d_{35} = 12\,218$ Ns/m,
$k_{53} = 135\,707$ N/m, $d_{53} = 12\,218$ Ns/m,
$k_{56} = 1000$ N/m, $d_{56} = 447$ Ns/m,
$k_{37} = 900\,000$ N/m, $d_{37} = 38\,500$ Ns/m.

The geometry constants are

$a_{13} = 2.0625$ m, $b_{34} = 0.279$ m,
$a_{23} = 2.4375$ m, $b_{43} = 0.946$ m,
$a_{35} = 1.9375$ m, $c_{35} = 0.800$ m,
$a_{34} = 1.8125$ m, $c_{53} = 0.900$ m,
$a_{43} = 3.0375$ m, $c_{56} = 0.200$ m,
$a_{53} = 3.6375$ m, $e_{37} = 2.435$ m,
$a_{37} = 0.9825$ m, $e_{z1} = 1.610$ m,
$a_{z1} = 3.0625$ m, $e_{z2} = 0.750$ m,
$a_{z2} = 0.1500$ m, $h_{eq} = 0.900$ m.

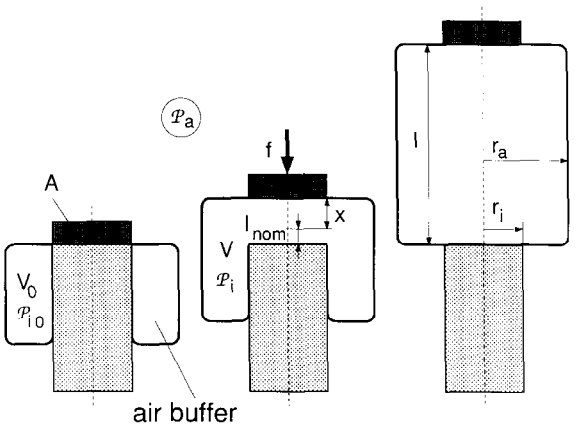

Fig. 5. Pneumatic spring.

The parameters $F_{eq,j}$ can be computed by solving a linear system in $F_{eq,j}$ and λ_0 for the static equilibrium $\ddot{p} = \dot{p} = p = 0$.

Nonlinear suspension elements

The special nonlinear suspension elements represent pneumatic springs, see Fig. 5. Their force law is given by

$$f_j(x_j) = (F_{eq,j} + \mathcal{P}_a A)\left(\frac{1 + s\, l_{nom,j}}{1 + s(x_j + l_{nom,j})}\right)^{\kappa} - \mathcal{P}_a A, \quad j = 13, 23.$$

The pneumatic spring coefficients are

$l_{nom,13} = 0.160$ m, $\quad \mathcal{P}_a = 1.0 \cdot 10^5$ Pa,
$l_{nom,23} = 0.160$ m, $\quad s = 39.1328$ m^{-1},
$l = 0.360$ m, $\quad \kappa = 1.4$,
$A = 0.0562$ m^2, $\quad d_{13} = 21\,593$ Ns/m,
$\quad d_{23} = 38\,537$ Ns/m.

Road excitation

For the excitation u at time $t_0 - t_1$ (rear wheel) and $t_0 - t_2$ (front wheel), we choose

$$t_0 = 0.0, \qquad t_1 = 0.15, \qquad t_2 = 0.0,$$

which corresponds to a velocity of $v_0 = 30$ m/s. The excitation is obtained by a Fourier series approximation of driveway measurements and an additional exponential damping factor. It can be evaluated by (units is [m])

$$u(t) = 0.01\left(\tfrac{1}{2}\alpha_0 + \sum_{i=1}^{10} \alpha_i \cos(2\pi i t\gamma) + \beta_i \sin(2\pi i t\gamma)\right)\exp\left(-0.1(t-7)^2\right).$$

The coefficients α_i, β_i, γ are

$$\alpha_0 = -8.523\,809\,523\,809\,5 \cdot 10^{-2},$$
$$\alpha_1 = 1.278\,739\,002\,588\,6 \cdot 10^{-1}, \qquad \beta_1 = 3.285\,154\,332\,660\,5 \cdot 10^{-3},$$
$$\alpha_2 = 7.038\,344\,124\,993\,2 \cdot 10^{-4}, \qquad \beta_2 = -3.924\,702\,169\,047\,5 \cdot 10^{-1},$$
$$\alpha_3 = 3.104\,830\,205\,341\,1 \cdot 10^{-1}, \qquad \beta_3 = -2.136\,662\,746\,053\,5 \cdot 10^{-1},$$
$$\alpha_4 = -3.370\,689\,475\,736\,1 \cdot 10^{-1}, \qquad \beta_4 = 1.202\,354\,177\,785\,2 \cdot 10^{-1},$$
$$\alpha_5 = 2.152\,497\,889\,828\,3 \cdot 10^{-1}, \qquad \beta_5 = 6.209\,259\,111\,147\,7 \cdot 10^{-2},$$
$$\alpha_6 = -2.036\,035\,135\,272\,5 \cdot 10^{-1}, \qquad \beta_6 = 4.251\,207\,200\,392\,7 \cdot 10^{-1},$$
$$\alpha_7 = 3.097\,619\,047\,619\,0 \cdot 10^{-1}, \qquad \beta_7 = -2.445\,490\,783\,067\,4 \cdot 10^{-1},$$
$$\alpha_8 = -2.560\,249\,816\,298\,5 \cdot 10^{-1}, \qquad \beta_8 = -4.088\,166\,042\,033\,6 \cdot 10^{-1},$$
$$\alpha_9 = -6.426\,045\,938\,781\,3 \cdot 10^{-2}, \qquad \beta_9 = 9.239\,563\,643\,601\,2 \cdot 10^{-2},$$
$$\alpha_{10} = -6.049\,549\,921\,263\,7 \cdot 10^{-2}, \qquad \beta_{10} = 7.465\,459\,922\,646\,9 \cdot 10^{-2},$$
$$\gamma = 1.904\,761\,904\,761\,9 \cdot 10^{-1}.$$

References

[1] V. Brasey and E. Hairer, Half-explicit Runge–Kutta methods for differential-algebraic systems of index 2, *SIAM J. Numer. Anal.* **30** (1993) 538–552.

[2] K.E. Brenan, S.L. Campbell and L.R. Petzold, *Numerical Solution of Initial-Value Problems in Differential-Algebraic Equations* (North-Holland, Amsterdam, 1989).

[3] E. Eich, C. Führer, B. Leimkuhler and S. Reich, Stabilization and projection methods for multibody dynamics, Technical Report, Helsinki Univ. Technology, 1990.

[4] C. Führer and B.J. Leimkuhler, Numerical solution of differential-algebraic equations for constrained mechanical motion, *Numer. Math.* **59** (1991) 55–69.

[5] F. Grupp and W. Kortüm, Parameter identification of nonlinear descriptor systems, in: W. Schiehlen, Ed., *Advanced Multibody System Dynamics — Simulation and Software Tools*, Stuttgart, 1993, Solid Mech. Appl. **20** (Kluwer, Dordrecht) 457–462.

[6] E. Hairer and G. Wanner, *Solving Ordinary Differential Equations II* (Springer, Berlin, 1991).

[7] C. Lubich, h^2 extrapolation methods for differential-algebraic systems of index 2, *Impact Comput. Sci. Engrg.* **1** (1989) 260–268.

[8] B. Simeon, An extended descriptor form for the numerical integration of multibody systems, *Appl. Numer. Math.* **13** (1–3) (1993) 209–220.

[9] B. Simeon, C. Führer and P. Rentrop, Differential-algebraic equations in vehicle system dynamics, *Surveys Math. Indust.* **1** (1991) 1–37.

[10] J. Stoer and R. Bulirsch, *Introduction to Numerical Analysis* (Springer, New York, 2nd ed., 1993).